

DESIGN AND VALIDATION OF AN ON-THE-GO SOIL STRENGTH PROFILE SENSOR

S. O. Chung, K. A. Sudduth, J. W. Hummel

ABSTRACT. Soil strength has traditionally been determined using the cone penetrometer, an instrument that provides highly variable discrete point measurements, making it difficult to detect statistically significant differences in the soil strength profile among treatments or locations. Generally, this problem has been addressed by obtaining a large number of measurements, a process that is time-consuming and labor-intensive. Our objective was to develop a soil strength profile sensor (SSPS) that could take measurements continuously and more efficiently while traveling across the field. The on-the-go SSPS was designed and fabricated using an array of load cells, each of which was interfaced with a soil-cutting tip. These multiple prismatic tips were extended forward from the leading edge of a vertical blade and spaced apart to minimize interference from the main blade and adjacent sensing tips. Prismatic soil strength index (PSSI, MPa) was defined as the force divided by the base area of the sensing tip. The sensing tip had a 60° cutting or apex angle and a base area of 361 mm². The design maximum operating depth was 0.5 m, and the upper limit and resolution of soil strength were 19.4 and 0.14 MPa, respectively. Field tests determined that the optimum extension and spacing of the cutting tips were 5.1 and 10 cm, respectively. A significant ($\alpha = 0.01$) linear relationship between PSSI and penetrometer cone index (CI), with a slope of approximately 0.6, was found for field data collected at a 30 cm depth. The ability to develop such relationships comparing penetrometer and SSPS data will allow SSPS data to be interpreted with respect to the available body of penetrometer literature.

Keywords. Cone penetrometer, Precision agriculture, Sensor, Soil compaction, Soil strength.

Site-specific crop management (SSCM) has been studied and increasingly adopted in many countries throughout the world. Soil properties are some of the most important information sources for SSCM because soil physical and chemical properties govern the transport of nutrients and water in the soil and the amount of plant-available nutrients and water (Barber, 1984). Compaction, a soil physical property, is a concern in crop production and environmental pollution. Soil compaction often restricts root development and growth (Lipiec and Stepniewski, 1995) due to increased bulk density and/or strength of the soil (Guerif, 1994), reduces the biological activity of plant roots and organisms in the soil due to reduced aeration (Voorhees et al., 1975), and limits water infiltration. The causes of soil

compaction and the resulting soil deformations may be different in the various soil layers (i.e., top layer, arable layer, and subsoil) (Koolen and Kuipers, 1983). Therefore, quantifying spatial and vertical variability in soil compaction and related soil properties would be useful in SSCM.

The degree of soil compaction, called compactness, traditionally has been determined through laboratory tests of soil samples and expressed as pore space, void ratio, or bulk density (Koolen and Kuipers, 1983). An alternative approach to estimate the state of soil compaction is to measure soil strength, since soil strength is strongly associated with compactness, packing density, relative bulk density, and drainable porosity (Canarache, 1991). Laboratory determination of either soil compactness or soil strength at the spatial resolution needed in SSCM is time-consuming, laborious, and expensive even if the required, spatially dense sampling is possible.

To overcome the limitations of laboratory tests, field sensors such as cone penetrometers (Mulqueen et al., 1977) have been developed to quantify soil properties related to soil compaction or soil strength. The index of soil strength measured by a cone penetrometer, cone index (CI), is defined as the force per unit base area required to push the penetrometer through a specified small increment of soil depth (ASAE Standards, 2005a, 2005b). Cone penetrometer readings require a “stop-and-go” procedure and only provide data at discrete locations, making it difficult to collect the amount of data required for SSCM. Even in nonspatial analyses, researchers have often used hundreds of penetrometer readings to investigate treatment differences (Busscher et al., 1986) and to relate cone index to soil properties such as water content and bulk density (Sojka et al., 2001). In

Article was submitted for review in December 2004 as manuscript number pm5689; approved for publication by the Power & Machinery Division of ASABE in January 2006. Presented at the 2003 ASAE Annual Meeting as Paper No. 031071.

Mention of trade names or commercial products in this article is solely for the purpose of providing specific information and does not imply recommendation or endorsement by the USDA or the National Institute of Agricultural Engineering, Republic of Korea.

The authors are **Sun-Ok Chung, ASABE Member Engineer**, Agricultural Engineering Researcher, National Institute of Agricultural Engineering, Rural Development Administration, Suwon, Korea; **Kenneth A. Sudduth, ASABE Member Engineer**, Agricultural Engineer, and **John W. Hummel, ASABE Fellow Engineer**, Agricultural Engineer, USDA-ARS Cropping Systems and Water Quality Research Unit, University of Missouri, Columbia, Missouri. **Corresponding author:** Kenneth A. Sudduth, USDA-ARS Cropping Systems and Water Quality Research Unit, University of Missouri, 269 Agricultural Engineering Bldg., Columbia, MO 65211; phone: 573-882-4090; fax: 573-882-1115; e-mail: sudduthk@missouri.edu.

contrast to penetrometer measurements, tillage draft measurements (Van Bergeijk et al., 2001) can provide the dense data needed for SSCM, but not with a high degree of precision, since draft is an integration of force over the operating depth and width of the tool, rather than a measurement of soil strength at a single soil depth and location.

A number of researchers have attempted continuous measurement of soil strength at multiple depths. An instrumented chisel was developed using a strain gauge array (Glancey et al., 1989) and used to predict draft requirements of tillage implements (Glancey et al., 1996). Data collected for comparison with sensor measurements included bulk density, water content, and cone index profiles to a 305 mm depth. Force distribution over the tillage depth was linear at a shallow operating depth (153 mm) in both tilled and untilled soils, while the distribution was nonlinear at a greater depth of operation (305 mm) in untilled soil. Similarly, Adamchuk et al. (2001) instrumented a vertical blade with an array of four strain gauges to map both horizontal and vertical spatial variation in mechanical soil resistance. By using a strain gauge array, these systems could predict soil cutting-force distribution over tool operating depths. A drawback of this approach was that the strain gauge array detected the deformation or bending moment of the tool, not the soil strength itself, making it difficult to calibrate and validate the effect of tool geometry.

Andrade et al. (2001) developed a soil cutting-force profile sensor that could take measurements up to a 63 cm depth on a 7.5 cm increment (5 cm active cutting elements separated by 2.5 cm dummy elements). The device consisted of eight cutting edges supported by independent load cells that measured the force on each cutting edge as the system was pulled through the soil. The soil cutting force was influenced by soil water content, depth of operation of the tine, and location of the cutting edge. Later evaluation of the sensor showed that the effect of operating speed on cutting force was not significant between 0.65 and 1.25 m s⁻¹ and that the sensor output could be expressed as a function of CI and operating depth with a coefficient of multiple determination of 0.985 (Andrade et al., 2002). One potential issue with this sensor design was the possibility that interactions between the adjacent cutting edges and between the main blade and cutting edges would affect the sensed soil strength.

Alihamsyah et al. (1990) and Alihamsyah and Humphries (1991) developed a horizontally operated penetrometer. Prismatic tips with different apex angles (20°, 25°, and 30°) and cone tips with different extensions from the main blade (0, 3, and 6 cm) were evaluated in three soil types (sandy loam, loam, and sand) and at two operating speeds (0.9 and 1.8 m s⁻¹). The prismatic penetrometer gave lower penetration resistance than the cone penetrometer in the sandy loam and loam but higher resistance in the sand. The effect of operating speed was not statistically significant. Resistance values generally increased with increasing tip extension from the main blade, except in the sand. The effect of apex angle was not consistent among different soil types, but measurements obtained using the prismatic penetrometer with an apex angle of 30° related well to CI.

Chukwu and Bowers (2005) modified the horizontally operating penetrometer developed by Alihamsyah et al. (1990) so that it could measure soil mechanical impedance at three depths simultaneously. They utilized three prismatic

tips with a 30° apex angle and three load cells similar to the one used in the single tip sensor. A 10 cm vertical tip spacing was chosen to provide a 30 cm sensing profile and to minimize measurement interference from one tip to the next. When operated at a speed of 0.03 m s⁻¹ through soil layered with different compaction levels, the sensor detected the difference in soil mechanical impedance with depth at a 5% significance level.

Researchers in Alabama (Raper and Hall, 2003; Hall and Raper, 2005) developed a device to measure soil strength on-the-go at different depths. The device had a sensor mounted on the leading edge of a tine and a reciprocating drive for oscillating the tine up and down while it was passing horizontally through the soil. They used 30° prismatic sensing tips and defined a “wedge index” as the measured force divided by the base area of the tips. With a 6.25 cm² wedge tip, CI was 1.52 times greater than the wedge index with an r² of 0.65. When the base area of the tip was increased to 25 cm², the slope of the relationship increased to 2.99 (r² = 0.83). They stated that an absolute equation to relate the wedge index and CI measurements might not be possible, since both measurement methods were empirical and were affected differently by different soil factors.

Previously developed on-the-go soil strength sensors have differed in: (1) the type of soil strength measured, i.e., bending stress on a tine (Adamchuk et al., 2001) and “CI-like” soil penetrating resistance (Andrade et al., 2001); (2) the number of sensing elements or depths, i.e., single (Alihamsyah et al., 1990) and multiple (Chukwu and Bowers, 2005); and (3) the shape and extension of sensing tips, i.e., 30° conical extended tip (Alihamsyah et al., 1990) and 30° prismatic flush-mounted tip (Raper and Hall, 2003). Although these prototype sensors have been able to provide on-the-go soil strength data, they are all still in development and testing stages. Advantages and disadvantages have been reported for each approach, and additional efforts in sensor development are warranted to obtain “CI-like” measurements with a soil-penetrating tip in an efficient manner. Testing such a sensor under various soil and operating conditions is necessary for better interpretation of the sensor measurements and developing applications for sensor data.

OBJECTIVES

The overall objective of this research was to design and validate an on-the-go soil strength profile sensor (SSPS) that could measure “CI-like” soil strength at multiple depths while traveling across a field. Specific objectives were:

- Design and construct the SSPS using an array of load cells based on the information obtained from our previous work in preliminary data analysis (Chung and Sudduth, 2004) and soil failure modeling (Chung and Sudduth, 2003).
- Conduct preliminary tests to optimize the sensor for reliable data acquisition and operation, including design of appropriate overload protection and evaluation of attachments to enhance penetration of the sensor into the soil.
- Investigate the effects of sensing tip extension (four extensions: 1.3, 2.5, 3.8, and 5.1 cm) and spacing (four spacings: 5, 10, 15, and 20 cm) at two operating speeds (0.5 and 1.0 m s⁻¹) and two depths (10 and 30 cm) through controlled field tests.

- In field tests, investigate relationships between soil strength measured by the SSPS and CI values obtained at corresponding depths.

MATERIALS AND METHODS

DESIGN AND CONSTRUCTION

The SSPS design concept enabled measurement of soil strength at multiple depths (fig. 1). Each force-sensing tip interfaced with a load cell located inside a narrow soil-cutting blade and was extended in front of the blade edge. The main blade was mounted to a frame using a shear bolt mechanism, and the frame was attached to a tractor through the three-point hitch. Major design issues were: (1) soil strength sensing, (2) data acquisition and calibration, (3) selection of materials for the main blade and sensing tip, and (4) tractor attachment and overload protection. Results obtained from our previous work in preliminary data analysis and soil failure modeling were used as guidelines for sensor design:

- Maximum sensing depth, expected maximum soil strength, and sensing resolution were selected as 50 cm, 10 MPa, and 0.1 MPa, respectively, based on examination of CI profiles from a Missouri claypan soil field (Chung and Sudduth, 2004). Higher loads due to dynamic operation of the sensor, along with a safety factor, were considered for appropriate load cell selection and sensor design. The desired maximum vertical sensing interval was 10 cm, contingent on being able to obtain accurate strength data from tips on that spacing.
- High-resolution and high-frequency data acquisition was needed to capture variability in soil strength. Assuming a 2 m s^{-1} normal operating speed, a minimum sampling frequency of 4 Hz was selected to detect repeating spatial patterns in CI (e.g., wheel traffic patterns). Faster data acquisition would be desirable for more reliable measurements and would allow application of filtering techniques such as a moving average (Chung and Sudduth, 2004).
- A prismatic tip with a 60° cutting or apex angle was selected as the sensing tool to reduce soil disturbance and avoid extreme force measurements for most soils, based on modeling and simulation of soil failure mechanisms (Chung and Sudduth, 2003).

Load Cell Selection

Load cell selection was based on the size and design of the sensing tip and the expected maximum values of soil resistance. A square bar was selected for fabrication of the prismatic sensing tip so that the base area of the tip, 361 mm^2 , was similar to that of the ASAE Standard large cone (323 mm^2 ; ASAE Standards, 2005a). A prismatic soil strength index (PSSI, MPa) was defined as the force measured by the SSPS divided by the base area of the prismatic tip, making it comparable to the CI (MPa) of a cone penetrometer. Assuming that PSSI would be less than 10 MPa in most agricultural soils at depths shallower than 50 cm, the maximum expected force was calculated as $10 \text{ MPa} \times 361 \text{ mm}^2 = 3.61 \text{ kN}$. After a survey of available commercial products, a miniaturized circular load cell with a diameter of 12.7 mm (model 8402, Burster GmbH, Gernsbach, Germany) was selected. The sensor had a full bridge circuit of foil strain gauges with temperature compensation from 15°C to 70°C .

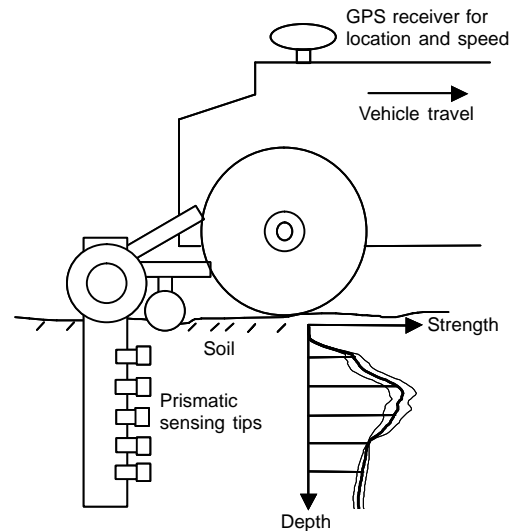


Figure 1. Operational concept of the on-the-go soil strength profile sensor.

Static capacity, dynamic capacity, and accuracy (combined non-linearity, hysteresis, and non-repeatability) of the load cell were 0 to 10 kN, 0 to 7 kN, and better than 50 N (0.5% of full scale), respectively. Corresponding PSSI values were 27.7, 19.4, and 0.14 MPa, respectively.

Main Blade and Prismatic Tip

Figure 2 (left) shows the unassembled structure of the soil strength sensor as viewed from the top: the body plate and cover plate comprising the main blade, the load cells and prismatic tips for strength sensing, and the retaining bar used to keep the prismatic tips from pulling out of the blade during operation. Detailed part drawings are given in Chung (2004). Materials were selected based on the design 50 cm sensing depth, durability, and machinability. The main blade consisted of two $86 \times 18 \text{ cm}$ stainless steel (AISI No. 17-4PH) plates ($\sigma_y = 758 \text{ MPa}$, $\sigma_t = 1,034 \text{ MPa}$); a 1.91 cm thick body plate, and a 0.63 cm thick cover plate. The body plate was machined to create pockets for the load cells, wiring tunnels, and grooves for the prismatic tips and retaining bar (fig. 2, center). With the cover plate installed, the blade was 2.54 cm thick and the front edge had a cutting angle of 60° . To create each prismatic tip, one end of a stainless steel (AISI No. 304) square bar ($\sigma_y = 276 \text{ MPa}$, $\sigma_t = 568 \text{ MPa}$, $1.9 \times 1.9 \text{ cm}$) was machined to an apex angle of 60° (fig. 2, right). The tip shaft was machined so that its size was smaller than that of the tip base to minimize the effect of shaft friction on the soil strength measurements.

A strength analysis was conducted to determine the optimum size of the tip-holding groove in the main blade, based on the relationship between a side force acting at the bottom of the blade and the corresponding bending stress at the groove. The shapes of the main blade and the groove were simplified to a cantilever beam and a rectangular cavity, respectively. The analysis showed that the main blade would endure a 35.7 kN side force without a cavity, and the allowable side force was decreased by only about 6% with a 10 mm wide rectangular groove. Based on this analysis, we selected the width of the cavity in the blade and the corresponding shaft of the prismatic tip as 8.3 mm. We selected the height of the cavity and shaft as 12.7 mm to provide adequate relief from the height of the prismatic tip, minimizing soil contact with the shaft during operation.

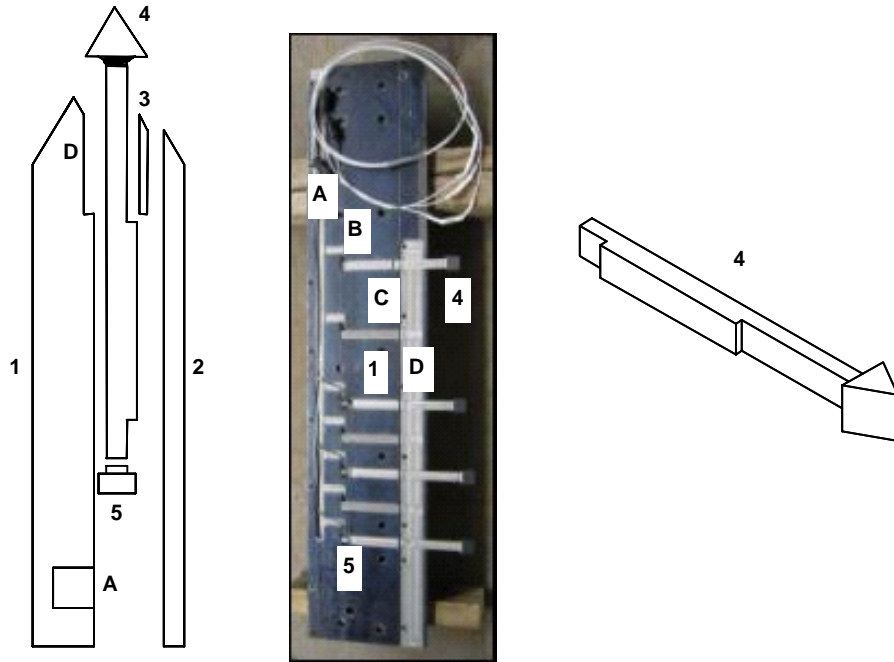


Figure 2. Structure of the soil strength sensor (not to scale): top view (left), side view of the body plate (center), and prismatic tip (right). Components include: (1) body plate, (2) cover plate, (3) retaining bar, (4) prismatic tip with 1.9×1.9 cm base area, and (5) load cell. Parts of the body plate include: (A) wiring tunnel, (B) holes for load cells, (C) grooves for prismatic tips, and (D) groove for retaining bar.

Mounting and Protection

A hitch frame was fabricated following the Category II specifications for a three-point free-link hitch (ASAE Standards, 2005c) to mount the soil strength sensor to an agricultural tractor. The frame had supporting wheels to set maximum operating depth and a disk coultter to cut plant residues and weeds in front of the sensor. The heights of the supporting wheels and disk coultter were adjustable for flexible operation of the sensor. Observations indicated that changes in sensing depth during field operation were generally less than 2 cm, which we judged to be acceptable. However, operation in heavy residue or soft soil conditions could cause this variability to increase to the point that continuous measurement of sensing depth would be required.

A shear bolt mechanism was devised to protect the load cells and blade (or hitch frame) from excessive loads. To design this mechanism, a stress, linearly increasing with soil depth from 0 MPa at the ground surface to 10 MPa at the lower end of the blade, was assumed to act on the blade. These loadings were chosen because 10 MPa was the expected maximum soil strength and 0 MPa was a reasonable boundary condition at the ground surface. Using these forces, the dimensions of the blade, and the standard double-shear equation, the required diameters of the shear bolt to resist the assumed force were 20.4 mm and 18.2 mm for SAE Grade 5 and Grade 8 bolts, respectively (Chung, 2004).

Data Acquisition

Force data for each tip were processed in parallel through a series of data acquisition components. The output of the Burster 8402 load cell was 1.5 mV V^{-1} at rated load (10 kN). A 3 V excitation input was used, resulting in a 4.5 mV signal at 10 kN. The signal from each load cell was sent to a data acquisition system (DaqBook/100, Iotech, Inc., Cleveland, Ohio) through a transducer amplifier (model S7DC, RDP Electrosense, Inc., Pottstown, Pa.). The amplifier provided a

variable gain, which was set at its maximum value of 1,250 for this application, and low-pass filtering with a 20 Hz bandwidth. The data acquisition system had a 100 kHz, 12-bit, 16-channel, 10 V A/D converter and a programmable gain setting function (set at a value of 2 for this application). Data from the DaqBook/100 were transmitted to a laptop computer through the parallel port. During field data collection, position information was obtained simultaneously from a DGPS receiver (approx. 1 m accuracy) through the computer's serial port.

Using the manufacturer's specifications, the output of the data acquisition system (as a digital number, DN) was transformed to a theoretical force (kN) and a theoretical PSSI (MPa):

$$\begin{aligned} \text{Force (kN)} &= \frac{\text{DN}}{R_{da} \times G_{da} \times G_{lc} \times V_{in}} \quad (1) \\ &= 2.17 \times 10^{-3} \text{ DN} \end{aligned}$$

where

R_{da} = data acquisition system resolution, 4096 counts $(10 \text{ V})^{-1}$

G_{da} = data acquisition system gain, 2500

G_{lc} = load cell gain, $1.5 \times 10^{-3} \text{ V V}^{-1}$ $(10 \text{ kN})^{-1}$

V_{in} = load cell input voltage, 3 V

$$\begin{aligned} \text{PSSI (MPa)} &= \frac{\text{force(kN)} \times 10^{-3}}{A_{tip}} \\ &= 2.77 \times \text{force(kN)} \\ &= 6.01 \times 10^{-3} \text{ DN} \quad (2) \end{aligned}$$

where A_{tip} is the projected area of the sensing tip ($3.61 \times 10^{-4} \text{ m}^2$).

Design Optimization

Preliminary field tests were conducted to verify the performance of the sensor and to determine if modifications were needed to enhance the reliability of the sensor under field conditions. The main concerns addressed in these tests were overload in the case of excessive soil resistance and penetration of the sensor into the soil.

The initial sensor design of a simple vertical blade was not able to penetrate the soil and achieve operating depth within a reasonable travel distance. To improve penetration, an aggressive suction foot was added; however, this caused excessive draft forces and shear bolt failure in high-strength soil conditions. After several modifications (Chung, 2004), a configuration that provided acceptable penetration without requiring excessive draft force was attained. This revised configuration included: (1) a less aggressive, 30° rake angled, 3.8 × 7.6 cm suction foot; (2) a revised main blade with the overall length reduced to 57 cm and the lower edge angled backward approximately 10° to reduce the surface area of the blade bottom in contact with the soil; and (3) the addition of approximately 180 kg of weight to the sensor mounting frame. With these revisions, the sensor could penetrate to the full operating depth (i.e., 50 cm) after 3 to 5 m of forward travel. Because the residue-cutting disk coulter was rigidly attached to the sensor frame, field operation required removal of crop residues from this short section at the start of each sensor run. A revised sensor design incorporating a floating coulter mechanism would be needed for more efficient sensor operation in large-scale data collection.

EXPERIMENTAL DESIGN AND ANALYTICAL PROCEDURES

Laboratory Tests and Calibration

Laboratory tests were conducted (1) to verify performance of the selected load cells, and (2) to verify equations 1 and 2 by testing the output of each amplifier with known forces. A cylindrical laboratory test fixture with three equally spaced holes smoothly fitting to the load cells was fabricated. Initially, a cylindrical metal plate was put on top of the load cells and the zero-offset of the data acquisition system was adjusted. Then, five tractor weights were loaded and unloaded one by one. Forces applied by the weights were 0, 0.32, 0.66, 0.99, 1.32, and 1.64 kN. At each loading and unloading increment, each of the three load cells in the fixture was connected to all five of the amplifiers one by one, and the amplified load cell signal output was sampled at a 100 Hz rate for 20 s. In this way, the signals representing the total, known weight at each stage were routed through each amplifier and the resulting output was recorded. Accurate testing was not possible by merely pairing an individual amplifier with each load cell because the fraction of the calibration weight supported by each of the three load cells in the fixture was unknown and not likely to be equal.

The distribution of each output was examined to verify the stability of the load cell signal. For amplifier calibration, the total response of each amplifier was obtained by summing outputs from the three load cells for each loading stage, which resulted in six data points for each amplifier, corresponding to the six loading levels listed above. The REG procedure in SAS version 8.01 (SAS Institute, Inc., Cary, N.C.) was used to obtain a linear relationship between measured digital number and applied force.

Field Tests for Tip Extension and Spacing

One of the most important goals in the design of the sensor was to measure strength due only to the interaction of the soil with the prismatic tip, minimizing interference from the main blade and adjacent tips. Field tests were designed to investigate the effects of tip extension from the main blade edge and of the spacing between tips. Four tip extensions (1.3, 2.5, 3.8, and 5.1 cm) and four tip spacings (5, 10, 15, and 20 cm) were evaluated. Extension was varied by using prismatic tips with different shaft lengths, while spacing was varied by changing the placement of tips in the vertical blade.

Tests were conducted at University of Missouri South Farm on claypan soils of the Mexico series (fine, smectitic, mesic aeris Vertic Epiaqualfs). These soils are fine-textured, have high clay content in the subsoil, and are somewhat poorly drained. The test location was chosen based on a Veris-shallow electrical conductivity (EC_a) map, collected using the methods described by Sudduth et al. (2003). This area (60 × 25 m, outlined as a rectangle in fig. 3) was selected to have relatively uniform EC_a values, indicating relatively homogeneous soil texture. Within each tip configuration test area, four 46 cm deep soil cores were collected for soil water content and texture analyses. Surface soil texture was uniformly silt loam. Subsurface (30 to 50 cm) texture was silt loam with the exception of one sample classified as silty clay loam. Surface soil water content was 18% to 26% at the time of tip extension tests and had dried to 12% to 18% at the time

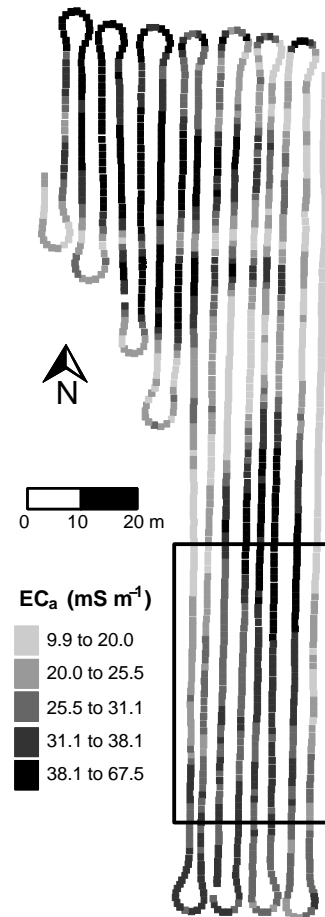


Figure 3. Locations of the field tests overlaid on a Veris-shallow EC_a map. Tests for determination of tip extension and spacing were conducted in the area outlined with a rectangle.

of tip spacing tests one week later. Subsurface (30 to 50 cm) soil water content was 20% to 24% for tip extension tests and 19% to 26% for tip spacing tests.

The main treatments (extension and spacing of tips) were randomly assigned. Two travel speeds (0.5 and 1.0 m s⁻¹) were achieved by adjusting the tractor gear and engine speed. For the tip extension tests, identical tips were placed at two depths (10 and 30 cm). For the tip spacing tests, one tip was placed at a constant depth of 30 cm and the depth of the other tip was varied from 10 to 25 cm to achieve the desired spacing. Data from the tips at both 10 cm and 30 cm were used in the extension tests. In the spacing tests, only data from the 30 cm depth was used, since the depth of the other tip was not constant among treatments. Six runs were conducted for each tip extension or spacing configuration (2 travel speeds × 3 replications).

The 1 m lateral spacing between the 25 m long runs was chosen to minimize the area required and thus the amount of soil variability encountered. For the tread width of the tractor used, this spacing meant that each successive sensor run was approximately 10 to 15 cm from the outside edge of the previous wheel track. Although near-surface compaction might be expected with this close proximity to wheel tracks, no such trend was identified when comparing CI profiles obtained adjacent to the sensor runs with other CI profiles centered between two sensor runs. The lack of measurable compaction near the wheel tracks may have been due to the relatively low axle weight of the tractor used, coupled with the dry soil conditions at the time of data collection. Even if

near-surface compaction was present, its effect should have been similar among all test runs since the placement of the runs with respect to wheel tracks was consistent.

Within each tip configuration test area, CI profiles were collected at six locations along the sensor test runs. The ASAE Standard large cone penetrometer system used for CI collection was developed by USDA-ARS at Columbia, Missouri. This self-contained, tractor-mounted, hydraulically powered device was equipped with five cone penetrometers equally spaced over 0.76 m. The five cone penetrometers could be inserted into the soil simultaneously, similar to the system developed by Raper et al. (1999). CI data were collected after, and with the array of penetrometers perpendicular to, the sensor test runs.

Issues investigated in these tests were: (1) effects of tip depth and operating speed, (2) comparison of PSSI and CI, and (3) effects of sensing tip extension and spacing. Procedures in SAS version 8.01 were used for analysis of variance (GLM), regression (REG), and Duncan's multiple range tests (MEANS). Typical graphs of CI versus depth and PSSI versus time are shown in figure 4. There were two penetrometer data collection sites for each sensor run (fig. 4); at each site, the mean of the five individual penetrometer traces was obtained and used for analysis. To more reliably compare PSSI with CI obtained at the same location, both signals were averaged. A 5 cm depth-averaged CI was calculated centered on each of the two tip operating depths, while a 2 m distance-averaged PSSI was calculated centered on each CI sampling position.

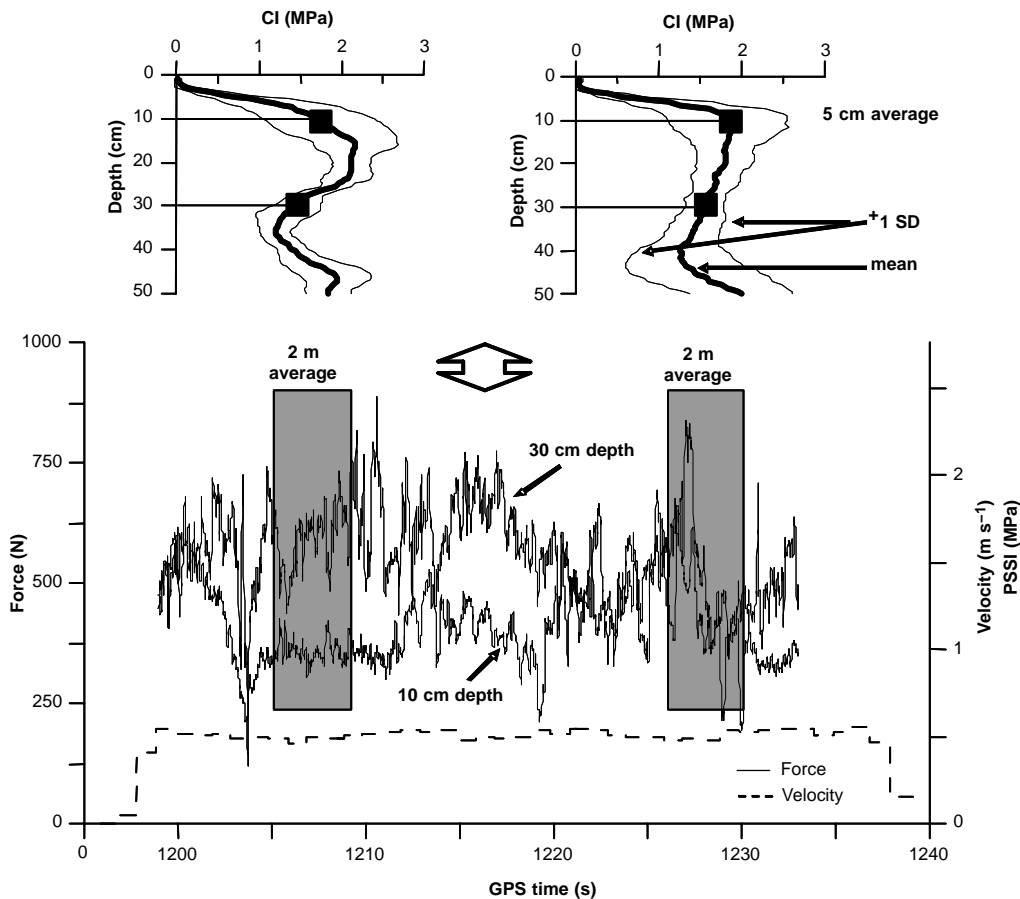


Figure 4. Typical CI and PSSI measurements. For reliable comparison of the measurements, 5 cm depth-averaged CIs and 2 m distance-averaged PSSI were used.

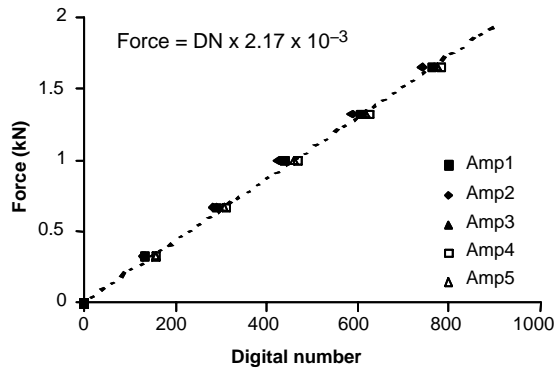


Figure 5. Relationship of applied static force to digital number (DN) in the load cell calibration tests.

RESULTS AND DISCUSSION

LABORATORY TESTS AND CALIBRATION

The output signals for static loading were normally distributed, as determined by the Kolmogorov-Smirnov statistic. The range and standard deviation were calculated from each output dataset collected for the different data acquisition channels and loadings. With a 95% confidence, the means of the ranges and standard deviations were 10.82 ± 0.29 DN and 1.44 ± 0.04 DN, respectively. From equation 2, the corresponding strength statistics were calculated as 0.065 ± 0.002 MPa and 0.009 ± 0.0002 MPa, respectively. These results verified that the load cells and data acquisition system were capable of recording reliable, low-noise signals in a static laboratory setting.

Figure 5 shows the linear response of the load cell/amplifier combination to the applied forces. The slope of the linear regression provided a calibration coefficient to relate the digital output of the system to the sensor force (or soil strength). When all data were combined into a single regression (y -intercept = 0, $\alpha = 0.05$), the empirical coefficient was the same as the theoretical coefficient given by equation 1. Although this overall slope coefficient differed by as much as 3% from individual amplifier slopes, we judged that the ability to interchange components for

troubleshooting or replacement justified the potential decrease in accuracy. Therefore, the theoretical coefficient of 2.17×10^{-3} was used to convert digital outputs (DN) to force measurements (kN), as shown in equation 1.

COMPARISON OF PSSI AND CI

Plots of PSSI versus CI showed a linear, positive relationship with slopes different from one (fig. 6). Based on dimensional analysis, Schuring and Emori (1964) found that the effects of soil inertia would not be significant at speeds less than $v = \sqrt{5gb}$, where g is acceleration due to gravity and b is tool width. Using the same approach, the critical speed of the SSPS ($b = 0.019$ m) was 0.97 m s⁻¹, close to the highest travel speed tested (1.0 m s⁻¹). Assuming no significant effects of operating speed, theoretical relationships between PSSI and CI would be linear for a given depth (Chung and Sudduth, 2003). Results of linear regression showed that the relationship was not significant at the 10 cm depth, but was significant at the 30 cm depth (table 1). The lack of statistical significance at the 10 cm depth was attributed to the small variation in soil strength, with a range in CI of less than 1 MPa (fig. 6, right). In contrast, CI at the 30 cm depth exhibited a range of 2.5 MPa or more (fig. 6). The slopes of the significant linear relationships at the 30 cm depth were about 0.6, indicating that, for these soils and under these test conditions, an increase in PSSI would be less than a corresponding increase in CI.

SELECTION OF TIP EXTENSION AND SPACING

The ratio of PSSI to CI was used to investigate the effect of extension and spacing of tips, since dividing PSSI by CI collected at the same location would help to remove the effects of other strength factors, such as soil conditions, which could vary by sampling location. The PSSI/CI ratio would be higher when a prismatic tip received less interference from the main blade and adjacent tips. Therefore, tip extensions and spacings that maximized this ratio were considered preferable. Data for the 2.5 cm extension were eliminated from the analysis due to apparent problems with that set of test runs. Figure 7 shows scatter plots of PSSI/CI

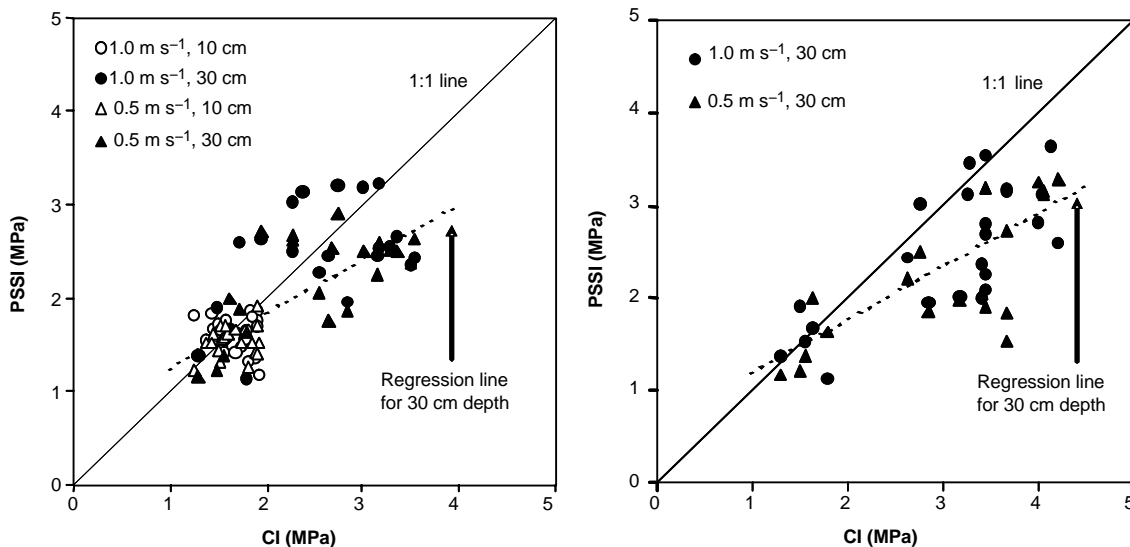


Figure 6. Plots of PSSI vs. CI data collected at different depths and travel speeds from the tests for extension (right) and spacing (left) of tips. Regression statistics are given in table 1.

Table 1. Results of linear regression of PSSI as a function of CI ($\alpha = 0.05$).

	Slope (P value)	y-Intercept (P value)	r^2
For extension			
10 cm depth	0.02 ± 0.33 (0.93)	1.53 ± 0.55 (<0.01)	0.01
30 cm depth	0.59 ± 0.18 (<0.01)	0.64 ± 0.48 (0.01)	0.60
For spacing			
30 cm depth	0.58 ± 0.17 (<0.01)	0.61 ± 0.53 (0.02)	0.54

ratio as functions of extension and spacing of sensing tips. For tip extension, the mean PSSI/CI ratio generally increased when extension increased from 1.3 to 3.8 cm; however, PSSI/CI ratio differences between the 3.8 and 5.1 cm extensions were not consistent among depths and operating speeds. For tip spacing, a clear increase in the ratio was found only when spacing was increased from 5 to 10 cm. These patterns of in-

creasing PSSI/CI ratio were similar for both the 0.5 and 1.0 m s^{-1} operating speeds.

Mean of the PSSI/CI ratio and its percent increase relative to the mean of the PSSI/CI ratio for the smallest tip extension and spacing are summarized in table 2. As observed in the scatter plots, general trends were: (1) means of the ratio increased with increasing extension and spacing of tips, and (2) the amount of increase was relatively large between the smallest level of extension or spacing and the next level, with increases ranging from 12% to 29%. Increases in soil strength measurements with larger tip extensions were also observed in sandy loam and loam soils by Alihamsyah and Humphries (1991).

For subsequent data collection, we selected a 5.1 cm tip extension because: (1) the PSSI/CI ratio was greatest (table 2), indicating the least interference, and (2) the increased extension did not compromise the strength of the

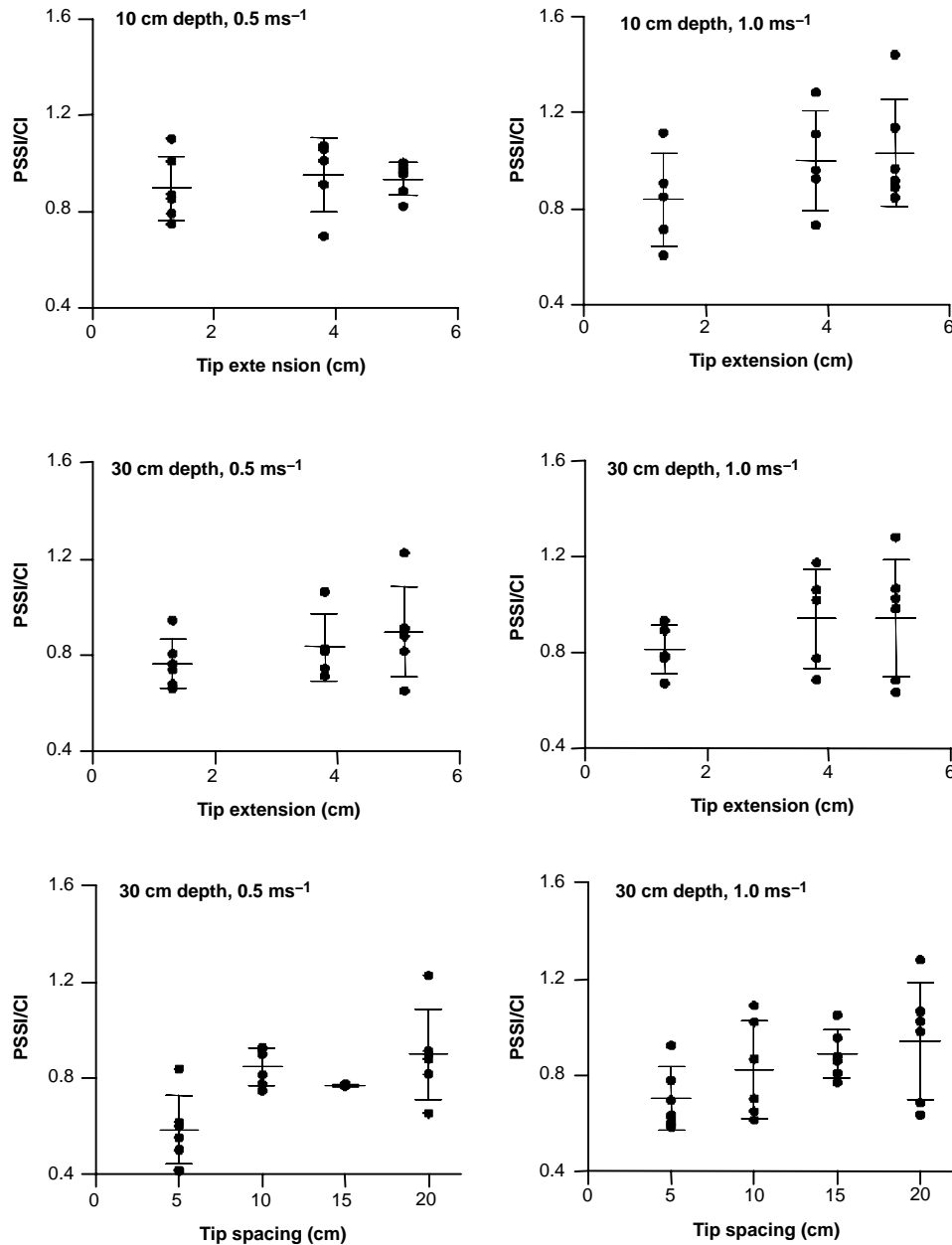


Figure 7. Plots of PSSI/CI vs. tip extension and PSSI/CI vs. tip spacing. Error bars in the plots indicate mean ± 1 standard deviation.

Table 2. Summary of tests to determine optimum extension and spacing of sensing tips.

Level	PSSI/CI Ratio		No. of Observations
	Mean	% Increase ^[a]	
For extension, 10 cm depth			
5.1 cm extension	0.985	13	12
3.8 cm extension	0.977	12	10
1.3 cm extension	0.870	—	11
For extension, 30 cm depth			
5.1 cm extension	0.921	17	12
3.8 cm extension	0.887	13	10
1.3 cm extension	0.786	—	11
For spacing, 30 cm depth			
20 cm spacing	0.921	43	12
15 cm spacing	0.858	33	8
10 cm spacing	0.835	29	12
5 cm spacing	0.645	—	12

^[a] Relative to smallest tip extension or spacing within each grouping.

tip/shaft system, with no bending observed during the field tests. We selected a 10 cm tip spacing as a compromise between reducing the interference between tips and maintaining adequate vertical resolution. Although mean PSSI/CI ratios were slightly higher (10% or less) for the 15 and 20 cm spacings compared to the 10 cm spacing (table 2), we decided that maintaining a 10 cm vertical resolution was more important than eliminating all potential interference from adjacent tips. The 10 cm tip spacing was also used by Chukwu and Bowers (2005).

The initial development and evaluation of the SSPS, as reported in this article, is promising. In limited field testing, data obtained with the sensor were linearly related to CI data obtained with an ASAE Standard cone penetrometer at a 30 cm depth and travel speeds of 0.5 and 1.0 m s⁻¹. Additional field testing will be required to validate this relationship across a range of soil types and to examine the effects of texture, water content, and bulk density. With the ability to acquire high-resolution soil strength data, the SSPS should be useful for a number of site-specific crop management applications, such as delineation of compacted areas for site-specific tillage, assessment of variability in soil strength and subsequent correlation of this variability with crop growth and yield, and integration with other sensing technologies (e.g., soil electrical conductivity) to provide enhanced *in situ* estimates of soil properties.

SUMMARY AND CONCLUSIONS

An on-the-go soil strength profile sensor (SSPS) that can obtain “CI-like” measurements at multiple depths continuously while traveling across the field has potential for research and production use. A prototype SSPS was developed and validated in laboratory and field conditions. Major findings were:

- The soil strength profile sensor used multiple prismatic tips, connected to a load cell array, extended horizontally in front of a main blade, and spaced apart from each other. The sensing tip had a 60° cutting or apex angle and a base area of 361 mm², which was comparable to the base area of the ASAE Standard large cone penetrometer. The design maximum operating depth was 0.5 m, and the upper limit and resolution of soil

strength were 19.4 and 0.14 MPa, respectively. A sensor-mounting frame was constructed and attached to an agricultural tractor using the three-point hitch, and a DGPS receiver was used for positional information.

- A data acquisition system was developed to collect signals from the load cells and DGPS receiver. Signals from the load cell array were filtered using a low-pass filter with a 20 Hz bandwidth, and collected using a 100 kHz, 12-bit, 16-channel, 10 V A/D converter. System output (digital number) was linear as a function of applied force in laboratory tests.
- Preliminary tests were conducted to optimize the SSPS in field conditions. Added weight (180 kg) and a 30° rake angled, 3.8 × 7.6 cm suction foot were used to enhance penetration of the sensor to the maximum operating depth of 0.5 m.
- The effects of extension and spacing of sensing tips were investigated through field tests at two speeds (0.5 and 1.0 m s⁻¹) and multiple operating depths. Based on these results, tip extension and spacing for further tests were chosen as 5.1 and 10 cm, respectively.
- Much of the variability in PSSI was explained by CI, and these two soil strength indices were linearly related for a given depth and speed. Regression showed that the linear relationship was not significant at the 10 cm depth, but was significant at the 30 cm depth, with a slope of about 0.6.

ACKNOWLEDGEMENTS

This research was supported in part by the North Central Soybean Research Program and the United Soybean Board, USA, and the International Cooperative Research Program, Rural Development Administration, Republic of Korea. The authors appreciate the contributions of Scott Drummond to development of the computer interface and data processing software, and of Joel Haden, Dale Clark, and Robert Mahurin to fabrication of the sensor.

REFERENCES

- Adamchuk, V. I., M. T. Morgan, and H. Sumali. 2001. Application of a strain gauge array to estimate soil mechanical impedance on-the-go. *Trans. ASAE* 44(6): 1377-1383.
- Alihamsyah, T., and E. G. Humphries. 1991. On-the-go soil mechanical impedance measurements. In *Proc. 1991 Symp. Automated Agric. for the 21st Century*, 300-306. St. Joseph, Mich.: ASAE.
- Alihamsyah, T., E. G. Humphries, and C. G. Bowers, Jr. 1990. A technique for horizontal measurement of soil mechanical impedance. *Trans. ASAE* 33(1): 73-77.
- Andrade, P., U. Rosa, S. K. Upadhyaya, B. M. Jenkins, J. Aguera, and M. Josiah. 2001. Soil profile force measurements using an instrumented tine. ASAE Paper No. 011060. St. Joseph, Mich.: ASAE.
- Andrade, P., S. K. Upadhyaya, B. M. Jenkins, and A. G. S. Filho. 2002. Evaluation of the UC Davis compaction profile sensor. ASAE Paper No. 021185. St. Joseph, Mich.: ASAE.
- ASAE Standards. 2005a. S313.3: Soil cone penetrometer. St. Joseph, Mich.: ASAE.
- ASAE Standards. 2005b. EP542: Procedures for using and reporting data obtained with the soil cone penetrometer. St. Joseph, Mich.: ASAE.
- ASAE Standards. 2005c. S217.12: Three-point free-link attachment for hitching implements to agricultural wheel tractors. St. Joseph, Mich.: ASAE.

- Barber, S. A. 1984. Nutrient uptake by plant roots growing in soil. In *Soil Nutrient Bio-availability: A Mechanistic Approach*, ch. 4. New York, N.Y.: John Wiley and Sons.
- Busscher, W. J., R. E. Sojka, and C. W. Doty. 1986. Residual effects of tillage on coastal plain soil strength. *Soil Sci.* 141(2): 144-148.
- Canarache, A. 1991. Factors and indices regarding excessive compactness of agricultural soils. *Soil Tillage Res.* 19(2-3): 145-164.
- Chukwu, E., and C. G. Bowers. 2005. Instantaneous multiple-depth soil mechanical impedance sensing from a moving vehicle. *Trans. ASAE* 48(3): 885-894.
- Chung, S. O. 2004. On-the-go soil strength profile sensor. PhD diss. Columbia, Mo.: University of Missouri.
- Chung, S. O., and K. A. Sudduth. 2003. Modeling soil failure caused by prismatic and conical tools. ASAE Paper No. 031028. St. Joseph, Mich.: ASAE.
- Chung, S. O., and K. A. Sudduth. 2004. Characterization of cone index and tillage draft data to define design parameters for an on-the-go soil strength profile sensor. *Agric. Biosystems Eng.* 5(1): 10-20.
- Glancey, J. L., S. K. Upadhyaya, W. J. Chancellor, and J. W. Rumsey. 1989. An instrumented chisel for the study of soil-tillage dynamics. *Soil Tillage Res.* 14(1): 1-24.
- Glancey, J. L., S. K. Upadhyaya, W. J. Chancellor, and J. W. Rumsey. 1996. Prediction of agricultural implement draft using an instrumented analog tillage tool. *Soil Tillage Res.* 37(1): 47-65.
- Guerif, J. 1994. Effects of compaction on soil strength parameters. In *Soil Compaction in Crop Production*, ch. 9, 191-214. B. D. Soane and C. Van Ouwerkerk, eds. Amsterdam, The Netherlands: Elsevier.
- Hall, H. E., and R. L. Raper. 2005. Development and concept evaluation of an on-the-go soil strength measurement system. *Trans. ASAE* 48(2): 469-477.
- Koolen, A. J., and H. Kuipers. 1983. *Agricultural Soil Mechanics*. Berlin, Germany: Springer-Verlag.
- Lipiec, J., and W. Stepniewski. 1995. Effects of soil compaction and tillage systems on uptake and losses of nutrients. *Soil Tillage Res.* 35(1-2): 37-52.
- Mulqueen, J., J. V. Stafford, and D. W. Tanner. 1977. Evaluating penetrometers for measuring soil strength. *J. Terramechanics* 14(3): 137-151.
- Raper, R. L., and E. H. Hall. 2003. Soil strength measurement for site-specific agriculture. U.S. Patent No. 6,647,799.
- Raper, R. L., B. H. Washington, and J. D. Jarrell. 1999. A tractor-mounted multiple-probe soil cone penetrometer. *Applied Eng. Agric.* 15(4): 287-290.
- Schuring, D. J., and R. I. Emori. 1964. Soil deforming processes and dimensional analysis. SAE Paper No. 897C. New York, N.Y.: SAE.
- Sojka, R. E., W. J. Busscher, and G. A. Lehrsch. 2001. In situ strength, bulk density, and water content relationships of a Durinodic Xeric Haplocalcic soil. *Soil Sci.* 166(8): 520-529.
- Sudduth, K. A., N. R. Kitchen, G. A. Bollero, D. G. Bullock, and W. J. Wiebold. 2003. Comparison of electromagnetic induction and direct sensing of soil electrical conductivity. *Agron. J.* 95(3): 472-482.
- Van Bergeijk, J., D. Goense, and L. Speelman. 2001. Soil tillage resistance as tool to map soil type differences. *J. Agric. Eng. Res.* 79(4): 371-387.
- Voorhees, W. B., D. A. Farrell, and W. E. Larson. 1975. Soil strength and aeration effects on root elongation. *Proc. Soil Sci. Soc. America* 39: 948-953.